

Probing R -parity Violating Interactions via $p\bar{p} \rightarrow e\mu + X$ Channel on Tevatron*

SUN Yan-Bin,¹ JIANG Yi,¹ HUANG Jin-Rui,¹ HAN Liang,¹ ZHANG Ren-You,¹ and MA Wen-Gan^{1,2}

¹Department of Modern Physics, University of Science and Technology of China, Hefei 230026, China

²CCAST (World Laboratory), P.O. Box 8730, Beijing 100080, China

(Received December 14, 2004)

Abstract We investigate the lepton flavor violation processes $p\bar{p} \rightarrow e\mu + X$ induced by R -parity violating interactions at the Tevatron hadron collider. The theoretical calculation and Monte Carlo simulation demonstrate that with a set of suitable cuts on experimental observables, one might be capable to reduce the standard model physical background to a controllable level so that the signals of R -parity violating interactions could be detected distinctively. Furthermore, clear sneutrino information can be abstracted from the purified event sample where other SUSY scalar quark “pollution” is heavily suppressed. We conclude that with a reasonable assumption of 10 fb^{-1} integrated luminosity, the experiments at the Tevatron machine would have potential to discover sneutrino in the region of $m_{\tilde{\nu}} \leq 400 \text{ GeV}$ via lepton flavor violation $e\mu$ production channels, or extend the mass scale constraint up to $m_{\tilde{\nu}} \geq 550 \text{ GeV}$ at 95% CL.

PACS numbers: 11.30.Fs, 11.30.Pb, 12.60.Jv, 14.80.Ly

Key words: lepton flavor violation, R -violating minimal supersymmetric standard model, hadron collider

1 Introduction

The observed neutrino oscillation^[1] implies strong lepton flavor violation (LFV). In the Standard Model (SM), lepton number is exactly preserved in contradiction with the neutrino oscillation. Some shortcomings of SM, for instance, the emergence of quadratic divergences in the Higgs sector, imply that SM needs to be extended. The Minimal Supersymmetric Standard Model (MSSM)^[2] is one of the most promising candidates in all extensions of SM. The most general superpotential in supersymmetry theory contains bilinear and trilinear terms which do not conserve either the baryon number (B) or the lepton number (L). The simultaneous presence of both lepton number violating and baryon number violating could lead to very rapid proton decay. In order to turn off proton rapid decay, supersymmetric models introduce a discrete R -parity symmetry^[3] implying a conserved quantum number $R = (-1)^{3B+L+2S}$, where B , L , and S are the baryon number, the lepton number, and the spin of particles, respectively. However, such a stringent symmetry appears short of theoretical basis. Especially we know that a stable proton can survive by imposing only one of L - and B -conservation. Moreover, non-zero R -violating couplings might provide small neutrino masses, which would explain the phenomena of neutrino oscillation experiments. Thus, there is strong theoretical and phenomenological motivation to introduce partial R -parity violations into the most general representations of superpotential, which can be written as^[4]

$$\begin{aligned} \mathcal{W}_{\not{R}_p} = & \frac{1}{2} \epsilon_{ab} \lambda_{ijk} \hat{L}_i^a \hat{L}_j^b \hat{E}_k + \epsilon_{ab} \lambda'_{ijk} \hat{L}_i^a \hat{Q}_j^b \hat{D}_k \\ & + \frac{1}{2} \epsilon_{\alpha\beta\gamma} \lambda''_{ijk} \hat{U}_i^\alpha \hat{D}_j^\beta \hat{D}_k^\gamma + \epsilon_{ab} \delta_i \hat{L}_i^a \hat{H}_2^b, \end{aligned} \quad (1)$$

where $i, j, k = 1, 2, 3$ are generation indices, $a, b = 1, 2$ are SU(2) isospin indices, and α, β, γ are SU(3) color indices. $\lambda, \lambda', \lambda''$ are dimensionless R -violating Yukawa couplings behaving as $\lambda_{ijk} = -\lambda_{jik}$, $\lambda''_{ijk} = -\lambda''_{jik}$. In the above superpotential, the last bilinear terms mix the lepton superfield and the Higgs one, which might generate masses of neutrinos and consequently introduce compatible description of neutrino oscillation in a natural way.^[5] All the other trilinear terms only violate either L - or B -symmetry respectively, and the terms that may produce both L - and B -violation simultaneously are forbidden in superpotential so that a stable proton is ensured.

Experimental detection on the signals of R -parity violating interactions would be the most outstanding evidence of new physics beyond the SM. If nature is supersymmetric and neutrino oscillations are really induced by R -violating couplings included in a general superpotential, then the prediction of single sneutrino production modes at colliders is straightforward. Therefore, probing single sneutrino production on a high-energy collider is specially attractive in experimental searches and relevant phenomenological studies about R -violating interactions. Such exploration ought to be promising if carried out on fine high-energy lepton colliders. There were some experimental bounds on LFV di-lepton cross-section measurement from LEP experiments,^[6] which can attribute to single sneutrino productions and will set mass constraint on these neutrino super-partners. We have discussed the possibility of probing off-shell sneutrino effect induced by $\hat{L}\hat{L}\hat{E}$ terms on a 500 GeV Linear Collider,^[7] and concluded that with current constraints on λ parameters one can extend sneutrino search up to $m_{\tilde{\nu}} \geq 1 \text{ TeV}$ region, which

*The project supported by National Natural Science Foundation of China and the Special Fund of the Chinese Academy of Sciences

is far beyond the constraints from LEP. Nevertheless, despite the high performance of Linear Colliders and clean environment in their detectors, none of TESLA, JLC or even ILC projects will be in commission in this decade. On the other hand, the Tevatron hadron collider is currently in its upgrade Run-II physics and the LHC will be put into running in three years, and consequently more careful studies on direct SUSY searches including the potential detection of single sneutrino production on hadron colliders should be addressed in detail both experimentally and phenomenologically.

The first two terms $\hat{L}\hat{L}\hat{E}$ and $\hat{L}\hat{Q}\hat{D}$ in the superpotential Eq. (1) may lead to R -violating single sneutrino production and sequential LFV decay on hadron colliders. Many papers studying these single sneutrino production modes both on- and off-mass-shell of sneutrino resonance via $\hat{L}\hat{Q}\hat{D}$ interactions and decay in R -parity conservation mode as $\tilde{\nu} \rightarrow l\tilde{\chi}_i^\pm$.^[8] Charginos and subsequential neutralinos can decay in R -conserving way as well, e.g. $\tilde{\chi}_i^\pm \rightarrow \tilde{\chi}_j^0 W^* \rightarrow \tilde{\chi}_j^0 l\nu$ and $\tilde{\chi}_j^0 \rightarrow \tilde{l}$; then sleptons from neutralino would decay in R -violating modes as $\tilde{l} \rightarrow l\nu$ or $\tilde{l} \rightarrow ud$. With these R -violating interaction vertexes involved in sneutrino and chargino/neutralino decay chains, single sneutrino will subsequently decay to all the SM stable particles at last. Namely, these single sneutrino production and subsequential χ^\pm/χ^0 decay processes are doubly R -violated, and unless light neutralinos would live long enough to escape from detectors there would be more than three leptons in final states. These characteristic triple-lepton signals are obviously good for tagging new physics. But there are problems in SUSY parameter determination from these multiple leptons channels: Firstly, the tri-lepton production can also be induced by R -conserving supersymmetric models, for instance, $\tilde{\chi}_i^\pm \tilde{\chi}_j^0$ associated production may have the subsequential decay to three leptons and two stable $\tilde{\chi}_1^0$ as the lightest supersymmetric particle (LSP), which performances as missing energy in detector. So, these tri-lepton channels might not be able to distinguish supersymmetric R -violating interaction signals from those of R -conserving ones. Secondly, since there are too many parameters involving in $\tilde{\nu} \rightarrow l\tilde{\chi}_i^\pm$ and chargino and neutralino cascade decay, it is complicated to determine any of SUSY parameters decisively, and one has to adopt a very compactly simplified version of parameters such as mSUGRA. On the contrary, the LFV di-lepton processes of sneutrino rare decay $\tilde{\nu} \rightarrow l_i^- l_j^+$ on hadron collider would provide an ideal detection channel for R -violating interactions and a potential means of abstracting some SUSY parameters experimentally. As we will show in the following sections with some reasonable assumption on parameter space and appropriate treatment on experimental observables, one is not only able to select LFV di-lepton signals

from numerous SM physics background, but also able to decouple the contribution of sneutrino part in signals from that of other SUSY parts, so that a unique sneutrino mass parameter could be abstracted explicitly.

Leaving alone the LHC in construction, Tevatron Run-II upgrade is now in progress. It is expected to deliver a proton-antiproton collision integrated luminosity as $\mathcal{O}(\text{fb}^{-1})$ per experiment at the energy of 1.96 TeV, which will be quantitatively one order higher than the luminosity acquired in Run-I with center of mass energy 1.8 TeV. Therefore, before LHC, the two experiments DØ and CDF on the Tevatron are the only available facilities to test R -violating interaction and search for sneutrino. In this paper, we will discuss the possibility of probing R -violating LFV di-lepton signals and abstracting sneutrino information from experimental observation at the Tevatron Run-II.

2 Analytical Expression on $e\mu$ Signal

We investigate two di-lepton signal processes in which final states can be identified precisely even in hadron colliding environment, namely $p\bar{p} \rightarrow q\bar{q}/\bar{q}q \rightarrow e^-\mu^+$ and its charge-conjugated process $p\bar{p} \rightarrow \bar{q}q/q\bar{q} \rightarrow e^+\mu^-$. By integrating the first two lepton number violation terms in Eq. (1), one can obtain the Lagrangian relevant to present discussion as

$$\begin{aligned} \mathcal{L}_f = & \frac{1}{2} \lambda_{ijk} (\bar{\nu}_{Li}^c e_{Lj} \tilde{e}_{jL}^* + e_{Li} \bar{\nu}_{Lj}^c \tilde{e}_{Rk}^* \\ & + \nu_{Li} e_{Lj} \bar{e}_{Rk} - e_{Li} \tilde{\nu}_{Lj} \bar{e}_{Rk}) \\ & \times \lambda'_{ijk} (\bar{\nu}_{Li}^c d_{Lj} \tilde{d}_{Rk}^* - e_{Ri}^c u_{Lj} \tilde{d}_{Rk}^* \\ & + \nu_{Li} \tilde{d}_{Lj} \bar{d}_{Rk} - e_{Li} \tilde{\nu}_{Lj} \bar{d}_{Rk} \\ & + \tilde{\nu}_{Li} d_{Lj} \bar{d}_{Rk} - \tilde{e}_{Li} u_{Lj} \bar{d}_{Rk}) + \text{h.c.}, \end{aligned} \quad (2)$$

where superscript c refers to charge conjugation. In this work, we simply take the R -violating parameters λ and λ' to be real to avoid further complication.

In order to get optimal efficiency of signal detection, we choose not to distinguish the absolute sign of lepton charge, so that di-track events of $e^-\mu^+$ final states will be treated equally as those of $e^+\mu^-$ ones. This summation treatment of $e\mu$ events[†] is based on the following consideration: Firstly, it can double the statistic of signal events, which will improve the significance and confidence on collected signal samples. Secondly, the charge determination of tracks with high transverse momentum (p_T) relies on many realistic detector-relevant factors, thus indiscrimination between $e^-(\mu^+)$ and $e^+(\mu^-)$ will remove systematic uncertainty on charge measurement. To reflect the summation measurement in theoretical calculation, we phenomenologically introduce a unique parton-level $\hat{\theta}$, to denote polar angles of both outgoing e^- and e^+ with respect

[†]The notation of charge-unspecified $e\mu$ denotes the summation of two final states $e^-\mu^+$ and $e^+\mu^-$ events.

to the incoming parton from proton beam, and adopt a consistent momentum notation to all signal processes as

$$q(p_1) + \bar{q}(p_2) \rightarrow e^-(p_3) + \mu^+(p_4), \quad (3)$$

$$q(p_1) + \bar{q}(p_2) \rightarrow e^+(p_3) + \mu^-(p_4), \quad (4)$$

$$\bar{q}(p_1) + q(p_2) \rightarrow e^-(p_3) + \mu^+(p_4), \quad (5)$$

$$\bar{q}(p_1) + q(p_2) \rightarrow e^+(p_3) + \mu^-(p_4), \quad (6)$$

where $q = u, d$ are the first-generation partons, p_1 stands for the four-momenta of partons from proton beam whose direction of vector \vec{p}_1 is along \hat{z} axis, and p_2 stands for those from anti-proton beam. We always use the four-momentum p_3 to denote outgoing e^- and e^+ in signal processes, so that the open angle between \vec{p}_3 and \vec{p}_1 is

precisely $\hat{\theta}$ defined above. Correspondingly, p_4 represents the four-momenta of final $\mu^+(\mu^-)$ particles. Neglecting electron and muon masses, we introduce Mandelstam invariant variables to describe kinematics of all the four signal subprocesses as

$$\hat{s} = (p_1 + p_2)^2 = (p_3 + p_4)^2,$$

$$\hat{t} = (p_1 - p_3)^2 = (p_2 - p_4)^2 = -\frac{\hat{s}}{2}(1 - \cos \hat{\theta}),$$

$$\hat{u} = (p_1 - p_4)^2 = (p_2 - p_3)^2 = -\frac{\hat{s}}{2}(1 + \cos \hat{\theta}), \quad (7)$$

and Feynman diagrams of $e\mu$ signals at parton level are depicted in Fig. 1 accordingly.

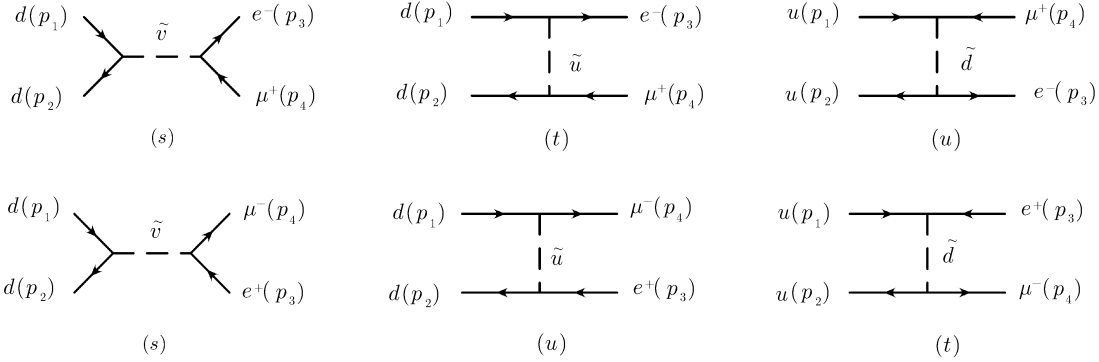


Fig. 1 The Feynman diagrams of subprocess $q\bar{q} \rightarrow e^\mp \mu^\pm$.

We define the amplitude of $d\bar{d} \rightarrow e^-\mu^+$ subprocess as $\mathcal{M}_{d\bar{d}}^{(-)}$, where the superscript minus sign in parenthesis indicates the processes with negative charged electrons in final states, and in the following we will use the superscript (+) to denote the processes with positive charged outgoing positrons. The amplitude $\mathcal{M}_{d\bar{d}}^{(-)}$ can be represented by \hat{s} - and \hat{t} -channel parts,

$$\mathcal{M}_{d\bar{d}}^{(-)} = \mathcal{M}_{d\bar{d}}^{(-)\hat{s}} - \mathcal{M}_{d\bar{d}}^{(-)\hat{t}} \quad (8)$$

with

$$\mathcal{M}_{d\bar{d}}^{(-)\hat{s}} = \sum_{i=1}^3 i \lambda_{i12} \lambda'_{i11} \bar{u}(p_3) P_R v(p_4) \mathcal{P}(\hat{s}, m_{\tilde{v}_i}) \bar{v}(p_2) P_L u(p_1) + (P_L \leftrightarrow P_R, \lambda_{i12} \lambda_{i11} \rightarrow \lambda_{i21} \lambda'_{i11}), \quad (9)$$

$$\mathcal{M}_{d\bar{d}}^{(-)\hat{t}} = \sum_{i=1}^3 \sum_{k=1}^2 -i \lambda'_{1i1} \lambda'_{2i1} |R_{1k}^{\tilde{u}_i}|^2 \bar{v}(p_2) P_L v(p_4) \mathcal{P}(\hat{t}, m_{\tilde{u}_{i,k}}) \bar{u}(p_3) P_R u(p_1), \quad (10)$$

and the notations of propagator factors $\mathcal{P}(x, m)$ are defined as follows:

$$\mathcal{P}(\hat{t}, m) = \frac{1}{\hat{t} - m^2}, \quad \mathcal{P}(\hat{u}, m) = \frac{1}{\hat{u} - m^2},$$

$$\mathcal{P}(\hat{s}, m) = \frac{1}{\hat{s} - m^2 + i\hat{s}\Gamma/m}, \quad (11)$$

where a sparticle width Γ is introduced into the \hat{s} -channel propagators to suppress resonance singularity. According to the Feynman diagrams in Fig. 1, the amplitude of $u\bar{u} \rightarrow e^-\mu^+$ subprocess has only \hat{u} -channel part and can

be denoted as

$$\mathcal{M}_{u\bar{u}}^{(-)} = \mathcal{M}_{u\bar{u}}^{(-)\hat{u}} \quad (12)$$

with

$$\mathcal{M}_{u\bar{u}}^{(-)\hat{u}} = \sum_{i=1}^3 \sum_{k=1}^2 -\frac{i}{2} \lambda'_{11i} \lambda'_{21i} |R_{2k}^{\tilde{d}_i}|^2 \bar{u}(p_4) P_L u(p_1) \times \mathcal{P}(\hat{u}, m_{\tilde{d}_{i,k}}) \bar{v}(p_2) P_R v(p_3). \quad (13)$$

In the above equation, $P_{L/R} = (1 \mp \gamma_5)/2$ are left- and right-hand project operators. $i(= 1, 2, 3)$ is generation index of supersymmetric particles, $k(= 1, 2)$ denotes the two mass eigenstates of each scalar quark flavor. $R^{\tilde{u}_i}$ and $R^{\tilde{d}_i}$

are the 2×2 matrices used to diagonalize various up and down-type squark mass matrices, respectively.

The amplitudes of the other type of signal subprocess $q\bar{q} \rightarrow e^+\mu^-$, represented by Eq. (4), can be written straightforwardly from the above expressions of Eq. (3) as

$$\begin{aligned}\mathcal{M}_{d\bar{d}}^{(+)\hat{s}} &= \mathcal{M}_{d\bar{d}}^{(-)\hat{s}}(p_3 \leftrightarrow p_4), \\ \mathcal{M}_{d\bar{d}}^{(+)\hat{u}} &= \mathcal{M}_{d\bar{d}}^{(-)\hat{t}}(p_3 \leftrightarrow p_4, \hat{t} \rightarrow \hat{u}), \\ \mathcal{M}_{u\bar{u}}^{(+)\hat{t}} &= \mathcal{M}_{u\bar{u}}^{(-)\hat{u}}(p_3 \leftrightarrow p_4, \hat{u} \rightarrow \hat{t}).\end{aligned}\quad (14)$$

The amplitudes of initial first-generation sea quark collision subprocesses, represented by Eqs. (5) and (6), can be obtained from those of valence incoming quark subprocesses of Eqs. (3) and (4) under the following replacement:

$$\begin{aligned}\mathcal{M}_{q\bar{q}}^{(\mp)\hat{s}} &= \mathcal{M}_{q\bar{q}}^{(\mp)\hat{s}}(p_1 \leftrightarrow p_2), \\ \mathcal{M}_{q\bar{q}}^{(\mp)\hat{u}} &= \mathcal{M}_{q\bar{q}}^{(\mp)\hat{t}}(p_1 \leftrightarrow p_2, \hat{t} \leftrightarrow \hat{u}), \\ \mathcal{M}_{q\bar{q}}^{(\mp)\hat{t}} &= \mathcal{M}_{q\bar{q}}^{(\mp)\hat{u}}(p_1 \leftrightarrow p_2, \hat{u} \leftrightarrow \hat{t}).\end{aligned}\quad (15)$$

By now all the signal amplitudes at parton level are given, where those of subprocess (3) are written explicitly, while those of the other three ones are obtained by appropriate initial and final states exchange respectively.

In this paper, we mainly focus on probing sneutrino resonance effect via potential LFV $e\mu$ signals at the Tevatron Run-II. Since the \hat{t} or \hat{u} -channel squark internal exchange diagrams contribute to signal measurement and

bring about ambiguity in exploring sneutrino information, which makes sense via the \hat{s} -channel exchange, we name all the squark contribution as ‘‘pollution’’ of the signal. Fortunately, because of the R -violating scalar-pseudoscalar (S-P) Yukawa couplings of fermion to Dirac fermions as shown in Eq. (2), the interference terms among \hat{s} -channel sneutrino exchange diagrams and \hat{t} and \hat{u} -channel squark interchange ones get vanished in all subprocesses. We call the vanishing of the interference terms between amplitudes of $\mathcal{M}^{(\mp)\hat{s}}$ and those of $\mathcal{M}^{(\mp)\hat{t}+\hat{u}}$, as a ‘‘decouple’’ feature between the two parts of sneutrino and squark contributions. In this way, we might be able to abstract sneutrino information from $p\bar{p} \rightarrow e\mu$ measurement. In order to reduce the number of parameters in sneutrino and squark sections, we simply take that the mass spectrum of all flavor scalar quarks is highly degenerated, and reasonably assume the mass splitting among three heavy sneutrinos is trivial so that a unique mass scale parameter could be introduced in the sneutrino section. That means

$$m_{\hat{u}_{i,k}} = m_{\hat{d}_{i,k}} = m_{\hat{q}}, \quad (16)$$

$$m_{\hat{\nu}_i} = m_{\hat{\nu}}. \quad (17)$$

To reflect the $e\mu$ summation and the decouple feature between sneutrino and squark contributions in the calculation of the signal production cross-section at hadron-level, we define a set of parton-level differential cross-section components as

$$d\hat{\sigma}_{qq'}^{\hat{s}} = \frac{1}{4} \frac{1}{9} \frac{N_c}{32\pi\hat{s}} |\mathcal{M}_{qq'}^{\hat{s}}|^2 d\cos\hat{\theta}, \quad (qq' = d\bar{d}, \bar{d}d), \quad (18)$$

$$d\hat{\sigma}_{qq'}^{\hat{t}+\hat{u}} = \frac{1}{4} \frac{1}{9} \frac{N_c}{32\pi\hat{s}} |\mathcal{M}_{qq'}^{\hat{t}+\hat{u}}|^2 d\cos\hat{\theta}, \quad (qq' = u\bar{u}, \bar{u}u, d\bar{d}, \bar{d}d), \quad (19)$$

where

$$|\mathcal{M}_{d\bar{d}}^{\hat{s}}|^2 = |\mathcal{M}_{d\bar{d}}^{\hat{s}}|^2 = |\mathcal{M}_{d\bar{d}}^{(-)\hat{s}}|^2 + |\mathcal{M}_{d\bar{d}}^{(+)\hat{s}}|^2 = 2 \times \hat{s}^2 |\mathcal{P}(\hat{s}, m_{\hat{\nu}})|^2 \sum_{i,i'=1}^3 \lambda'_{i11} \lambda'_{i'11} (\lambda_{i12} \lambda_{j12} + \lambda_{i21} \lambda_{j21}). \quad (20)$$

$$\begin{aligned}|\mathcal{M}_{d\bar{d}}^{\hat{t}+\hat{u}}|^2 &= |\mathcal{M}_{d\bar{d}}^{\hat{t}+\hat{u}}|^2 = |\mathcal{M}_{d\bar{d}}^{(-)\hat{t}}|^2 + |\mathcal{M}_{d\bar{d}}^{(+)\hat{u}}|^2 = [\hat{u}^2 \mathcal{P}(\hat{u}, m_{\hat{q}})^2 + \hat{t}^2 \mathcal{P}(\hat{t}, m_{\hat{q}})^2] \\ &\times \sum_{i,i'=1}^3 \sum_{k,k'=1}^2 (\lambda'_{1i1} \lambda'_{2i1} |R_{k1}^{\hat{u}_i}|^2 \lambda'_{1i'1} \lambda'_{2i'1} |R_{k'1}^{\hat{u}_{i'}}|^2),\end{aligned}\quad (21)$$

$$\begin{aligned}|\mathcal{M}_{u\bar{u}}^{\hat{t}+\hat{u}}|^2 &= |\mathcal{M}_{u\bar{u}}^{\hat{t}+\hat{u}}|^2 = |\mathcal{M}_{u\bar{u}}^{(-)\hat{u}}|^2 + |\mathcal{M}_{u\bar{u}}^{(+)\hat{t}}|^2 = [\hat{u}^2 \mathcal{P}(\hat{u}, m_{\hat{q}})^2 + \hat{t}^2 \mathcal{P}(\hat{t}, m_{\hat{q}})^2] \\ &\times \sum_{i,i'=1}^3 \sum_{k,k'=1}^2 (\lambda'_{21i} \lambda'_{11i} |R_{k2}^{\hat{d}_i}|^2 \lambda'_{21i'} \lambda'_{11i'} |R_{k'2}^{\hat{d}_{i'}}|^2).\end{aligned}\quad (22)$$

The above expressions manifest that with the summation treatment on $e\mu$ signal processes, the \hat{s} -channel contribution is doubled, while \hat{t} and \hat{u} -channel contributions always come together and will cancel their individual forward-backward distribution asymmetry on polar angle $\hat{\theta}$ with each other at parton level.

Due to the decouple feature between sneutrino and squark sections, we are safe to divide the calculation of $e\mu$ signal total cross-section at the Tevatron into two separate parts named as sneutrino and squark cross-section contributions, respectively, as

$$\sigma[p\bar{p} \rightarrow e\mu] = \sigma^{(\hat{\nu})} + \sigma^{(\hat{q})}. \quad (23)$$

And the differential cross-sections are

$$\frac{d^3\sigma^{(\tilde{\nu})}}{dx_1 dx_2 d\cos\hat{\theta}} = \sum_{qq'=d\bar{d},\bar{d}d} f_q^p(x_1, Q^2) f_{q'}^{\bar{p}}(x_2, Q^2) \frac{d\hat{\sigma}_{qq'}^{\hat{s}}(\hat{s} = x_1 x_2 s)}{d\cos\hat{\theta}}, \quad (24)$$

$$\frac{d^3\sigma^{(\tilde{q})}}{dx_1 dx_2 d\cos\hat{\theta}} = \sum_{qq'=u\bar{u},\bar{u}u} f_q^p(x_1, Q^2) f_{q'}^{\bar{p}}(x_2, Q^2) \frac{d\hat{\sigma}_{qq'}^{\hat{t}+\hat{u}}(\hat{s} = x_1 x_2 s)}{d\cos\hat{\theta}}. \quad (25)$$

We adopt the Pythia^[9] built-in parton distribution function (p.d.f) of the proton and antiproton, CTEQ5L, and implement the above hadron-level calculation by convoluting Eqs. (24) and Eq. (25) with 1.96 TeV $p\bar{p}$ collision energy. Here we should clarify that the above defined parton-level $\hat{\theta}$, which is the polar angle of outgoing $e^- (e^+)$ with respect to the incoming parton from proton beam, will be boosted to an experiment observable angle θ between $e^- (e^+)$ and proton beam. In this way, we get an event generator of LFV $e\mu$ production at the Tevatron based on the package Pythia. Now the question is, apart from the theoretical calculation, how we can find some appropriate observables in which the overlap of sneutrino and squark contribution parts is minimized, so that one can suppress squark pollution to a trivial level and abstract sneutrino information clearly from experiment.

3 Numerical Result and Discussion

We take the R -parity violating parameters λ and λ' under the experimental constraints presented in Ref. [10]. All the scale factors in the constraints, which are SUSY particle mass-dependent, are simply ignored, so that the R -violating Yukawa couplings could be naturally kept at values less than $\mathcal{O}(10^{-1})$. Thereby, there is only mass scale parameter $m_{\tilde{\nu}}$ in sneutrino section as free parameter which should be determined by experiment. The degenerate sneutrino mass parameter has to be constrained by the latest concrete LEP collider data. For example, OPAL experiment has set an upper limit on $\sigma(e^+e^- \rightarrow e\mu)$ as 22 fb with $200 \leq \sqrt{s} \leq 209$ GeV at 95% CL.^[6] To get a consistent value with this observation, one can arrive at^[7]

$$m_{\tilde{\nu}} \geq 250 \text{ GeV}. \quad (26)$$

A unique sneutrino decay width Γ is set to be 10 GeV, which results in a very short $\tilde{\nu}$ lifetime. The degenerate scalar quark mass is taken as $m_{\tilde{q}} = 100$ GeV except otherwise specified, and 2×2 $R^{\bar{u}}$ and $R^{\bar{d}}$ mixing matrices are set to be unit for simplification.

According to the decouple feature of sneutrino and squark section at parton level, we plot two independent contributions to the $e\mu$ signal production cross-section on $p\bar{p}$ collider at $\sqrt{s} = 1.96$ TeV, as the functions of the corresponding mass parameter $m_{\tilde{\nu}}$ and $m_{\tilde{q}}$, respectively, in Fig. 2. Due to the \hat{s} -channel resonance enhancement, the sneutrino contribution is dominant over the squark one in

most region of parameter space. However, on account of the less density of valence quark p.d.f in higher energy region, the resonance enhancement will decrease with the increment of sneutrino mass, and the cross section drops to a few femto barn in the vicinity of $\sqrt{\hat{s}} \sim m_{\tilde{\nu}} = 500$ GeV. The calculation shows as well that the cross-section at hadron level contributed by scalar quark exchange $\hat{t}+\hat{u}$ -channel is 5 fb when $m_{\tilde{q}} = 100$ GeV, and becomes negligible when $m_{\tilde{q}} \gg 100$ GeV.

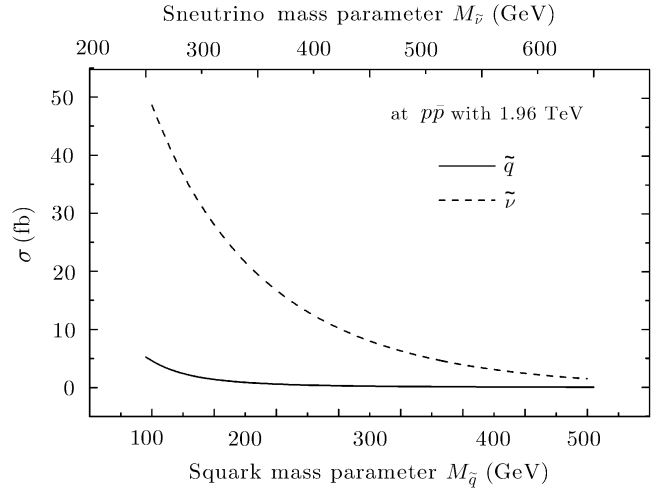


Fig. 2 The $e\mu$ signal production cross section parts contributed by sneutrino and squark sectors respectively, as the functions of $m_{\tilde{\nu}}$ and $m_{\tilde{q}}$ at the Tevatron Run-II.

A set of MC distributions of $e\mu$ signal observables at the Tevatron, i.e. polar angle $\cos\theta$, pseudo-rapidity $\eta = -\ln(\tan\theta/2)$, and transverse momentum p_T of outgoing electron, and invariant mass of $e\mu$ system are plotted in Fig. 3 with $m_{\tilde{\nu}} = 500$ GeV and $m_{\tilde{q}} = 100$ GeV, where the pollution from scalar quark section is maximized. The sneutrino contribution is characterized by the di-lepton invariant mass peak around $M_{e\mu} = \sqrt{\hat{s}} \sim m_{\tilde{\nu}}$, and the lepton transverse energy tendency as $E_T \sim m_{\tilde{\nu}}/2$, while the two leptons from squark section are much softer. Therefore, with a proper cut on $e\mu$ invariant mass, we ought to get rid of squark pollution and derive a purified sneutrino section. It should be clarified here that we adopt Eqs. (24) and (25) to generate the above two individual “virtual” MC event samples contributed by squark and sneutrino respectively, but will generate the “true” sam-

ples by using the differential cross-section contributed by both squark and sneutrino sections in following event se-

lection strategy studies.

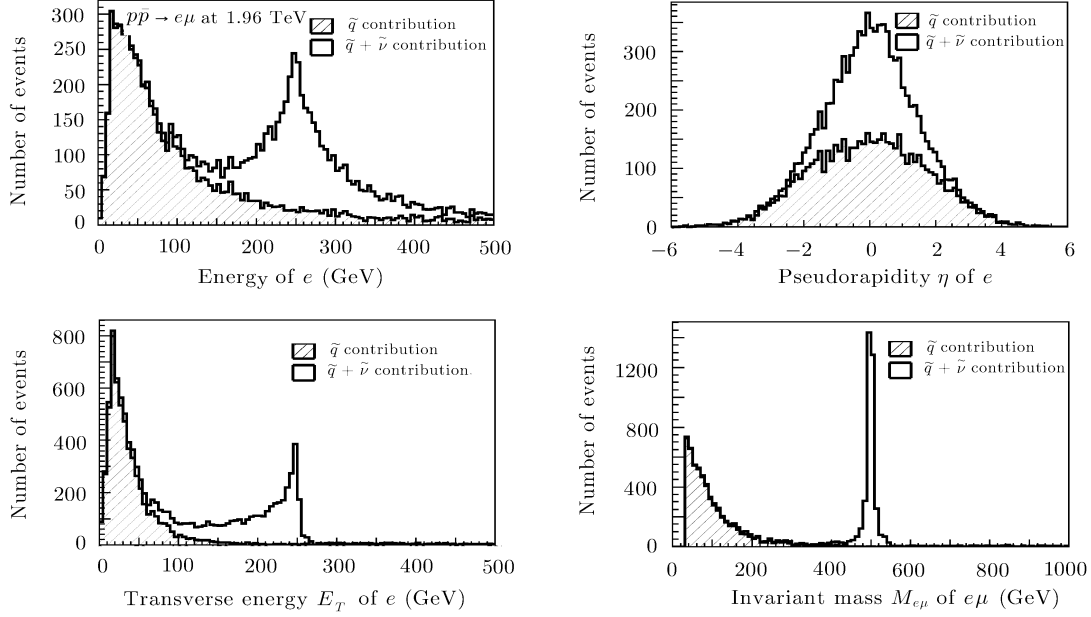


Fig. 3 MC distributions of $e\mu$ signal at the Tevatron Run-II. The hatched histograms are from squark section, and the unhatched histograms are given by squark + sneutrino section contribution.

For the background of the signal, we consider the following processes, which have significant $e\mu$ candidates in their final states,

$$p\bar{p} \rightarrow W^+W^-, \tau^+\tau^-, b\bar{b}, t\bar{t} \rightarrow e\mu + X,$$

where X refers to decay products of W , τ , b , and t other than $e\mu$. As discussed in Ref. [7], $b\bar{b}$ process can be removed by calorimeter-based energy isolation cut on both $e\mu$ candidates, for these leptons from b -quark semi-leptonic decay are very soft and always associated with charmed meson as $b \rightarrow qW^* \rightarrow jl\nu$. However, for $t\bar{t}$ events where top quark decays to bW exclusively, there are possible $e\mu$ final states from WW subsequential decay, together with b -quarks fragmented into two jets, which cannot be tagged easily. Different from e^+e^- collider case, these $t\bar{t}$ production events with $e\mu$ in final states accompanied by two b -quarks jets might not be distinguished from those signal events, in which besides $e\mu$ there are two jets produced by remnant parton collision or multiple interactions in high luminosity hadron collider environment. Therefore, there are three kinds of processes which should be taken into account as physical background, and the relevant cross-sections at the Tevatron Run-II are

$$\sigma_{WW} = \sigma[p\bar{p} \rightarrow W^+W^-] \times 2\text{Br}[W \rightarrow e\nu_e] \text{Br}[W \rightarrow \mu\nu_\mu] = 8.45 \text{ pb} \times 2 \times 11\% \times 11\% = 204.5 \text{ fb}, \quad (27)$$

$$\sigma_{tt} = \sigma[p\bar{p} \rightarrow t\bar{t}] \times 2\text{Br}[W \rightarrow e\nu_e] \text{Br}[W \rightarrow \mu\nu_\mu] = 8.32 \text{ pb} \times 2 \times 11\% \times 11\% = 201.3 \text{ fb}, \quad (28)$$

$$\sigma_{\tau\tau} = \sigma[p\bar{p} \rightarrow \tau^+\tau^-] \times 2\text{Br}[\tau \rightarrow e\nu_e\nu_\tau] \text{Br}[\tau \rightarrow \mu\nu_\mu\nu_\tau] = 229.67 \text{ pb} \times 2 \times 17\% \times 17\% = 13.27 \text{ pb}. \quad (29)$$

Some MC distributions of $t\bar{t}$ and $\tau\tau$ background are depicted in Figs. 4 and 5 respectively. Distributions of WW are very similar to those of $t\bar{t}$ and thus are not plotted here. These distributions show that in $t\bar{t}$ and WW events there are quite large missing transverse energy and non-collinearity of $e\mu$ in azimuthal plane, while $e\mu$ final states in $\tau\tau$ events are very soft and derive small invariant mass. These features of background are useful to developing an efficient event selection strategy to suppress background and improve the significance of signal.

Taking the advantage of the collinearity and the resonance effect of energetic $e\mu$ signal contributed by sneutrino section, we suggest the following off-line event selection strategy at Run-II Tevatron to reduce SM physical background as well as squark pollution.

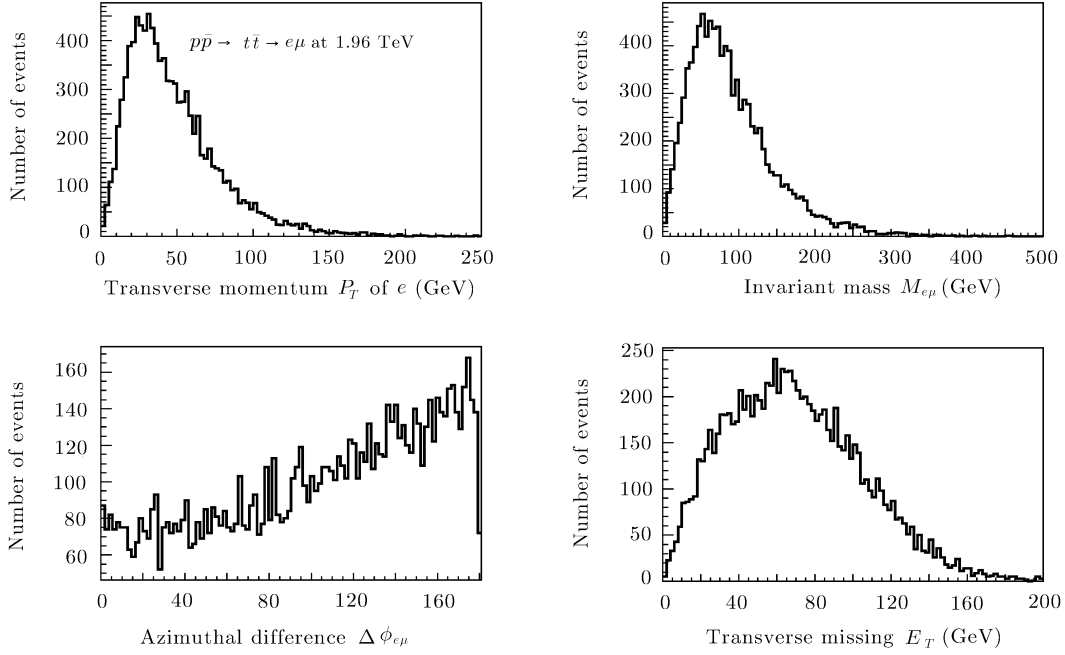


Fig. 4 MC distributions of the tt background.

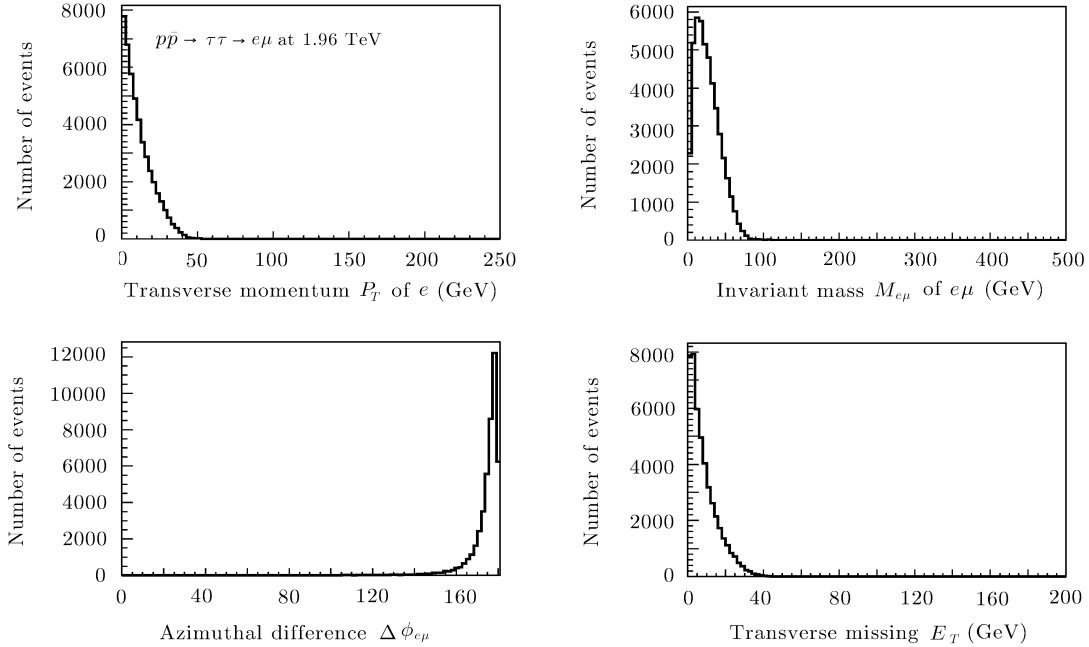


Fig. 5 MC distributions of the $\tau\tau$ events background.

(i) CUT1 Geometry Acceptance: Heavily boosted at the Tevatron, the pseudo-rapidity distribution of signals does not show distinct difference from those of background, namely all $e\mu$ candidates will tend to forward-backward distributed. Accordingly, we merely adopt the real detector acceptance on both signal and background to

avoid signal loss. For demonstration, we take the real geometry of upgraded DØ detector^[11] in simulation, where the pseudo-rapidity coverage of Muon+Tracker system is

$$|\eta| \leq 1.8 \ \& \ \text{NOT}[|\eta| \leq 1.25 \ \& \ 4.25 \leq \phi \leq 5.15], \quad (30)$$

and the coverage of the Central Calorimeter which pro-

vides better energy resolution than the two Endcap ones is

$$|\eta| \leq 1.2. \quad (31)$$

(ii) CUT2 Transverse Momentum constraint: In order to reject tremendous soft QCD jets which might produce counterfeit electron and muon simultaneously in high luminosity hadron collision environment, we use p_T cut on both electron and muon candidates as

$$p_T \geq 30 \text{ GeV}. \quad (32)$$

(iii) CUT3 Invariant Mass constraint: In order to remove the scalar quark pollution from total signals, we make an invariant mass cut as

$$M_{e\mu} \geq 140 \text{ GeV}, \quad (33)$$

which is just greater than half of 250 GeV, the current lower bound on sneutrino mass given in Eq. (26). We deliberately choose such a loose cut to leave room for resolution and uncertainty in real track transverse momentum and EM object energy scale measurement. In this way, $\tau\tau$ events will be suppressed heavily. Additionally, this invariant mass constraint will also be efficient on some instrumental background, e.g. single Z^0 production which decays via $Z^0 \rightarrow \mu^- \mu^+$, where one of its decay produced muons occasionally deposits nearly all its energy in Calorimeter and thus provides a fake electron candidate. However, a good-sized part of WW and $t\bar{t}$ events can survive after this cut yet.

(iv) CUT4 Collinearity constraint: Assuming high spatial resolution on x - y plane vertical to the beam, we

set a cut on $e\mu$ ϕ -difference to select back-to-back events as

$$165^\circ \leq \Delta\phi_{e\mu} \leq 180^\circ, \quad (34)$$

where we allow a 15° redundancy, considering that the remnant parton collisions recoiled in signal processes might carry some significant amount of transverse momenta in total.

(v) CUT5 Missing Transverse Energy constraint: In LFV signals there is not any missing \cancel{E}_T . However, in consideration of detector resolution we cut on a non-zero value as

$$\cancel{E}_T \leq 30 \text{ GeV}. \quad (35)$$

Four sets of MC samples for W^+W^- , $\tau^+\tau^-$, $t\bar{t}$ background and LFV signal productions with $m_{\tilde{\nu}} = 500$ and $m_{\tilde{q}} = 100$ GeV are generated by Pythia at the Tevatron Run-II $p\bar{p}$ collider with $\sqrt{s} = 1.96$ TeV, scaled with different assumed luminosity. Each sample is simulated with the five-step event selection, and the numbers of events passing individual CUT are listed in Table 1, respectively. Despite different assumed luminosity in generating the MC samples, we define a selection efficiency variable on both background and signal as

$$\epsilon = \frac{N_5}{N_0}. \quad (36)$$

It is demonstrated that with the five-step strategy we are able to reduce the background by 2 ~ 3 orders, i.e. $\epsilon_{WW} \sim 2.0\%$, $\epsilon_{t\bar{t}} \sim 0.6\%$, and $\epsilon_{\tau\tau} \sim 0.013\%$, while keeping the selection efficiency on the R -violating $e\mu$ signal as high as 27%.

Table 1 Event selection efficiency on background and signal. The first six rows are numbers of events before and after individual CUT. The values of event selection efficiency on different samples are given in the seventh row.

	SM background $W^+W^- \rightarrow e\mu$	SM background $\tau^+\tau^- \rightarrow e\mu$	SM background $t\bar{t} \rightarrow e\mu$	$e\text{-}\mu$ signal ($m_{\tilde{\nu}} = 500$ GeV, $m_{\tilde{q}} = 100$ GeV)
no cut N_0	9981	46 066	9996	99 952
CUT1 N_1	5163	13 575	6272	36 333
CUT2 N_2	2312	140	3357	31 702
CUT3 N_3	566	16	960	26 860
CUT4 N_4	262	16	317	26 860
CUT5 N_5	198	6	62	26 860
efficiency ϵ	2.0%	0.013%	0.6%	26.9%
σ before CUT	204.5 fb	13.27 pb	201.3 fb	9.16 fb
σ after CUT	4.09 fb	1.73 fb	1.21 fb	2.46 fb

With certain integrated luminosity L , the number of background events, B and that of $e\mu$ signal, S , dominated by the contribution of sneutrinos with $m_{\tilde{\nu}} = 500$ GeV after selection is given by

$$S = (\sigma_{e\mu} \cdot \epsilon_{e\mu})L = \sigma_{e\mu}^{\text{CUT}} \times L = 2.46 \text{ fb} \times L \quad (37)$$

$$\begin{aligned} B &= (\sigma_{WW}\epsilon_{WW} + \sigma_{\tau\tau}\epsilon_{\tau\tau} + \sigma_{t\bar{t}}\epsilon_{t\bar{t}}) \times L \\ &= \sigma_{\text{SM}}^{\text{CUT}} L = 7.03 \text{ fb} \times L, \end{aligned} \quad (38)$$

where $\sigma_{\text{SM}}^{\text{CUT}}$ is the sum of W^+W^- , $\tau^+\tau^-$, and $t\bar{t}$ contribution after CUTs, and $\sigma_{e\mu}^{\text{CUT}}$ is the cross-section of R -

violating LFV $e\mu$ signal. The significance of signal over background is defined as

$$SB = \frac{S}{\sqrt{B}} = \frac{\sigma_{e\mu}^{\text{CUT}}}{\sqrt{\sigma_{\text{SM}}^{\text{CUT}}}} \times \sqrt{L}. \quad (39)$$

In the following discussion, we optimistically assume some 10 fb^{-1} integrated luminosity would be accumulated at both the $D\emptyset$ and CDF experiment eventually, which is not an unreachable goal for the Tevatron Run-II luminosity upgrading is in progress remarkably. Accordingly, the significance of signal from 500 GeV sneutrino contribution is about 3.

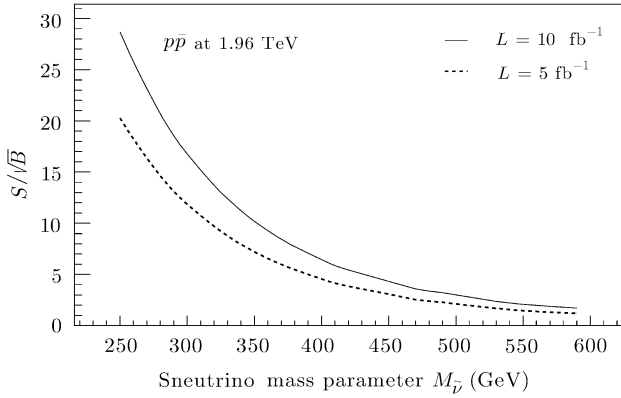


Fig. 6 The significance SB as a function of $M_{\tilde{\nu}}$ with $M_{\tilde{q}} = 100 \text{ GeV}$ at the Tevatron with different integrated luminosity estimates.

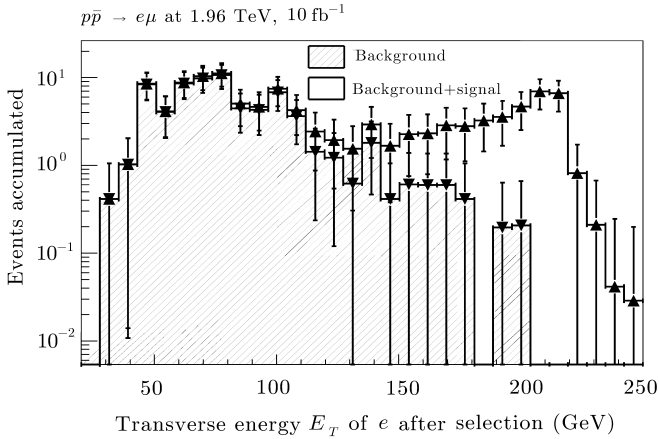


Fig. 7 Distributions of electron candidates after selection. The numbers are normalized with integrated luminosity 10 fb^{-1} . The hatched histogram is for SM background, and the unhatched one is background folded with 430 GeV sneutrino signal.

The significance SB as functions of sneutrino mass $m_{\tilde{\nu}}$ at the Tevatron is plotted in Fig. 6, with integrated luminosity being 5 fb^{-1} and 10 fb^{-1} respectively, where $L = 5 \text{ fb}^{-1}$ is taken as conservative estimate for reference. One can see clearly that LFV signals contributed by sneutrinos lighter than 430 GeV will derive significance of signal over the SM background greater than 5

for $L = 10 \text{ fb}^{-1}$, and thus will be detected explicitly. The signal cross-section dominated by the contribution of 430 GeV sneutrinos will hold as large as 4.2 fb after selection, and there will be some 40 signal events on record together with 70 background events in total 10 fb^{-1} data. The transverse energy distributions of selected electron candidates are plotted in Fig. 7. Despite trivial remnant of scalar quark pollution, the outstanding peak in higher region of selected electron E_T distribution denotes the half value of sneutrino mass scale, and reveals the R -violating single sneutrino production distinctively.

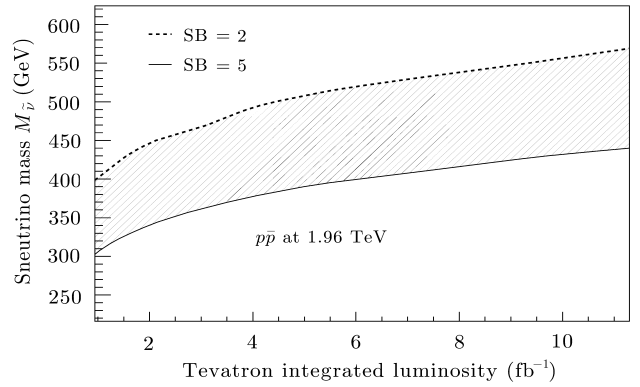


Fig. 8 Discovery ($SB = 5$, solid line) and exclusion ($SB = 2$, dot line) limits on sneutrino mass parameter as a function of the Tevatron integrated luminosity. The region between these two lines are those which cannot be excluded or discovered explicitly.

Figures 6 and 7 show that with an optimized 10 fb^{-1} luminosity recorded in total, LFV signals of degenerated sneutrinos with masses smaller than 400 GeV will be detected at the Tevatron at more than 5 significance, and an apparent precipitate structure shown in transverse energy distributions of selected electron candidates would reveal the whereabouts of sneutrino mass scale. The ratio of signal to background can be as large as 0.6, which is acceptable for a stable data analysis. Consequently, if the sneutrino mass scale really lies in the region of $m_{\tilde{\nu}} \leq 400 \text{ GeV}$, the $D\emptyset$ experiment at the Run-II Tevatron will discover these supersymmetric scalar partners of Dirac neutrinos via LFV $e\mu$ signal processes; while if no experimental evidence is observed, one can exclude sneutrino up to $m_{\tilde{\nu}} \geq 550 \text{ GeV}$ at 95% CL, where significance is smaller than 2. We adopt the criterion that the R -violating LFV signal is discovered at $SB > 5$ and excluded when $SB < 2$. Accordingly, figure 8 shows the discovery and exclusion regions of sneutrino as functions of integrated luminosity at the Tevatron. The solid and dotted curves correspond to the significance of the signal over background (SB) being 5 and 2, and thus the sneutrino mass parameter regions above or under the hatched area can be excluded or discovered, respectively.

4 Summary

We have studied the lepton flavor violation processes $p\bar{p} \rightarrow e\mu + X$ at the Tevatron Run-II with $\sqrt{s} = 1.96$ TeV colliding energy, in the framework of the R -parity violating MSSM. There are two types of R -violating interactions involved in the LFV signal processes, namely the couplings of sneutrino-lepton (quarks) vertices and those of squark-quark-lepton ones. Fortunately, due to the R -violating S-P Yukawa couplings of sfermion to Dirac leptons and quarks, the contribution of sneutrino section is decoupled with that of squark part. Accordingly, one is able to cut on an appropriate observable such as invariant mass $M_{e\mu}$ to remove most of scalar quark pollution, and derive sneutrino mass parameter from purified data sample which is

dominated by sneutrino contribution.

Making use of the sneutrino resonance effect and $e\mu$ collinearity in transverse plane vertical to beam pipe, we develop a set of event selection strategies. Under these strategies, the SM background can be under control, so that it is possible to probe the R -parity violating interactions and to abstract the sneutrino information from experimental observation. We conclude that with an assumption of 10 fb^{-1} integrated luminosity, the experiments at the Tevatron Run-II machine will have the potential to discover sneutrino in the region of $m_{\tilde{\nu}} \leq 400$ GeV by detecting LFV $e\mu$ signals, or extend the mass scale constraint up to $m_{\tilde{\nu}} \geq 550$ GeV at 95% CL within the MSSM framework with R -parity violation.

References

- [1] Y. Fukuda, *et al.*, Super-Kamiokande Collaboration, Phys. Lett. B **433** (1998) 9; Phys. Lett. B **436** (1998) 33; Phys. Rev. Lett. **81** (1998) 1562; M. Apollonio, *et al.*, Chooz Collaboration, Phys. Lett. B **420** (1998) 297.
- [2] H.P. Nilles, Phys. Rep. **1** (1984) 110; H.E. Haber and G. Kane, Phys. Rep. **117** (1985) 75.
- [3] P. Fayet, Phys. Lett. B **69** (1977) 489; G.R. Farrar and P. Fayet, Phys. Lett. B **76** (1978) 575.
- [4] S. Weinberg, Phys. Rev. D **26** (1982) 287; N. Sakai and T. Yanagida, Nucl. Phys. B **197** (1982) 533.
- [5] J.C. Romao, M.A. Diaz, M. Hirsch, W. Porod, and J.W. Valle, Phys. Rev. D **61** (2000) 071703; Phys. Rev. D **62** (2000) 113008.
- [6] G. Abbiendi, *et al.*, Phys. Lett. B **519** (2001) 23.
- [7] Y.B. Sun, L. Han, W.G. Ma, T. Farshid, R.Y. Zhang, and Y.J. Zhou, JHEP **0409** (2004) 043.
- [8] R. Barbieri, *et al.*, hep-ph/9810232; B. Allanach, *et al.*, hep-ph/9906224; F. Deliot, *et al.*, Phys. Lett. B **475** (2000) 184; G. Moreau, *et al.*, Nucl. Phys. B **604** (2001) 3; S. Bar-Shalom, *et al.*, Phys. Rev. D **64** (2001) 095008.
- [9] T. Sjöstrand, P. Edén, C. Friberg, L. Lönnblad, G. Miu, S. Mrenna, and E. Norrbin, Computer Phys. Commun. **135** (2001) 238 (LU TP 00-30, [hep-ph/0010017]).
- [10] R. Barbieri, *et al.*, [hep-ph/9810232]; B. Allanach, *et al.*, [hep-ph/9906224].
- [11] The DØ detector is described in detail elsewhere as T. LeCompte and H.T. Diehl, Ann. Rev. Nucl. Part. Sci. **50** (2000) 71; DØ Collaboration, S. Abachi, *et al.*, Nucl. Instrum. Methods Phys. Res. A **338** (1994) 185.